Density Functional Theory Study of Pyrrole Adsorption on Mo(110)

Wa'el A. Abdallah and Alan E. Nelson*

Department of Chemical and Materials Engineering, University of Alberta, Edmonton, Alberta T6G 2G6 Canada

The objective of the present study is to identify possible adsorption configurations of pyrrole on Mo(110) using density functional theory (DFT) calculations. Several adsorption configurations were studied including pyrrole and pyrrolyl adsorption as parallel, perpendicular, and tilted adsorption modes relative to the Mo-(110) surface plane. Based on the DFT calculations, pyrrole is suggested to adsorb in a parallel mode with respect to the Mo(110) surface through its π-orbital as μ_3,η^5-Pyr-0° with an adsorption energy of −28.7 to −31.5 kcal mol^{-1}. The possibility of a coexisting mode where pyrrole adsorbs on the surface with a slightly tilted molecular plane as μ_3,η^4(N,C2,C3,C4)-Pyr-5° is also likely to occur, particularly at higher pyrrole coverages. The slightly tilted configuration is suggested to arise from the lateral interactions of adsorbed pyrrole on Mo(110), and not the result of a phase transformation on the surface since this requires a relatively high activation energy as indicated by additional linear synchronous transit (LST)/quadratic synchronous transit (QST) calculations. Both adsorption geometries bond to three surface Mo atoms, and Mo(110) did not promote hydrogen abstraction. Pyrrolyl adsorption on Mo(110) is energetically possible, but unlikely to occur because gas-phase hydrogen has not been previously experimentally observed as a pyrrole decomposition product on Mo(110).

1. Introduction

Numerous experimental and theoretical studies have been reported investigating the adsorption and reaction of basic organonitrogen compounds, specifically pyridine and its derivatives, on model transition metal catalyst surfaces to understand the mechanistic features of hydrodenitrogenation (HDN) chemistry.[1−6] Although these studies have provided incremental gains in HDN catalyst activity, fundamental questions remain regarding nonbasic (pyrrole) organonitrogen adsorption on molybdenum-based hydrotreating catalyst surfaces. Pyrrole (C_4H_5N) is a nonbasic organonitrogen heterocycle in which the lone electron pair of nitrogen is delocalized over the π-system of the ring.[7,8] The lone-pair electrons of the nitrogen atom and the two C=C bonds form a six-electron conjugated π-electron system. This electronic configuration is suggested to result in strong pyrrole adsorption on molybdenum-based sulfided hydrotreating catalysts, but very little is known about the mode of adsorption.[9]

Organometallic chemistry has provided some information regarding the possible bonding modes of pyrrole to metal complexes.[10] Based on these studies, several different bonding configurations have been suggested, as summarized in Figure 1. The most numerous metal complexes of pyrrole are the η^5-Pyr type (Figure 1e), which are known for Cr, Mn, Fe, Co, Ru, Rh, Re, and Ir surfaces.[11−14] The η^4-Pyr type (Figure 1d) has been observed in one case, where the pyrrole ligand clearly bonded through the two C=C bonds, while the nitrogen atom is bent away from the ring to a nonbonding distance from the metal ion.[15] While there are no records of η^1(N)-Pyl ligand (Figure 1f), metal derivatives containing an olefin-like ligand, in either one of the tautomeric forms η^2(C=C)-H-Pyl (Figure

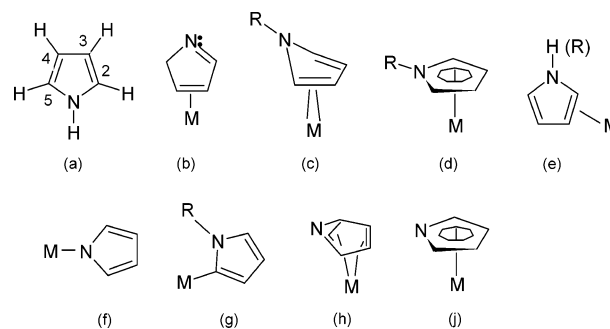
Figure 1. Summary of pyrrole bonding modes [adapted from ref 10]. (a) Gas-phase pyrrole; (b) η^2(C,C)-2H-Pyl; (c) η^2(C,C)-H-Pyl; (d) η^4-Pyr; (e) η^5-Pyr; (f) η^1(N)-Pyl; (g) η^1(C)-Pyl; (h) η^3,η^2-Pyl; (j) η^5-Pyl.

1c) or η^2(C=C)-2H-Pyl (Figure 1b), have been characterized for osmium(II) complexes.[16,17] Metal complexes containing the anionic pyrrolyl ligands are much more frequent throughout the periodic table, and the η^1(N)-Pyl (Figure 1f) and η^5-Pyr (Figure 1e) bonding modes are dominant in the coordination chemistry of such anions.[11,18] Depending on the degree of electronic unsaturation of the reacting metal containing fragment, the incoming pyrrolyl ligand binds through the N-atom only, or through the entire π-ring.

Because the mechanistic features of HDN reactions are not well-defined on a molecular level, studies of discrete metal−heterocyclic complexes have been carried out in order to investigate fundamental questions on how the heterocycle might interact with and be activated by a catalyst surface. We have previously investigated pyrrole adsorption on Mo(110) using temperature-programmed desorption (TPD) and Auger electron spectroscopy (AES),[19] and one molecular desorption feature was observed at several surface coverages. This molecular desorption feature was suggested to be the result of parallel or slightly tilted molecular pyrrole adsorption modes without cleaving any

* Corresponding author. Telephone: (780) 492-7380. Fax:(780) 492-2881. E-mail: alan.nelson@ualberta.ca.

hydrogen bonds. In this work, first-principles quantum mechanical calculations using density functional theory (DFT) are used to study the molecular adsorption of pyrrole on Mo(110) in an attempt to identify the adsorption configurations resulting in molecular desorption and surface decomposition, and to gain further insight about the structure−reactivity relationship.

2. Experimental Methods

2.1. Molecular Simulations. A commercial ab initio quantum mechanical package employing density functional theory (DFT) plane-wave pseudopotential methods (CASTEP, Accelrys) was used for all calculations. Geometry optimization for all systems including the Mo(110) surface and pyrrole was based on the BFGS algorithm scheme that has the ability to perform cell optimizations, in which the BFGS scheme uses a staring Hessian that is recursively updated during optimization. The BFGS algorithm adopts the exchange-correlation gradient-corrected functional GGA-PBE.[20] The exchange part of the Perdew−Burke−Ernzerhof functional (PBE) is designed to give results similar to that of the Perdew−Wang generalized-gradient approximation (PW91),[21] but it is more robust in systems with rapidly varying electron density. The quality of the electronic minimization was set using a kinetic cutoff energy of 270 eV with a Monkhorst−Pack[22] k-point mesh of $2 \times 2 \times 2$ and k-point spacing of 0.05 Å^{-1}. The tightly bound core electrons are represented by nonlocal ultrasoft pseudopotentials (USP) as proposed by Vanderbilt[23] to allow calculations to be performed with the lowest possible cutoff energy for the plane-wave basis set. The density mixing scheme was set with a self-consistent field tolerance of 1×10^{-6} eV/atom using the Pulay method,[24] in which the output density is mixed with densities from a number of previous iterations using the RMM-DIIS method leading to more rapid convergence. This computational basis has been used in our previous work.[3] A combination of linear synchronous transit (LST) and quadratic synchronous transit (QST) methods were used to find the transition state (TS) by setting the reaction pathway of the reactant and the product structures. The calculations used 10 images along the reaction path with a convergence tolerance set to fine quality (0.05 eV/Å) with a maximum of five QST steps.

2.2. Models and Energy Calculations. The Mo(110) surface was built from a bulk Mo crystal (bcc) and cleaved to expose the (110) crystallographic orientation. The Mo(110) surface with an area of 10.90 Å × 10.90 Å consisting of two atomic layers was placed in a vacuum supercell with a thickness of 12.22 Å to eliminate artificial interactions between the slabs. The surface geometry was refined to obtain a stable structure using an iterative process in which the coordinates of the atoms are adjusted so that the total energy of the structure is minimized. After surface minimization, a single optimized pyrrole molecule was placed inside the vacuum cell at an approximate distance of 2.2 Å from the molybdenum surface, similar to the bond distances observed in molybdenum organometallic complexes.[10] The second atomic layer from the bulk was constrained from interaction, and the model was allowed to optimize to calculate the total minimized energy for the molecular interaction with the surface. The adsorption energies, E_{ads}, of the different adsorption modes were calculated as

$$E_{ads} = E_{a+s} - (nE_a + E_s) \qquad (1)$$

where E_a is the energy of a gas-phase pyrrole molecule, n is the number of adsorbed pyrrole molecules per unit cell, E_s is

the energy of the relaxed Mo(110) substrate without the adsorbate, and E_{a+s} is the total energy of the relaxed Mo(110) surface with the adsorbate. Except for the coverage-dependent studies, a single pyrrole molecule was placed in the unit cell to eliminate lateral interactions with other pyrrole molecules.

3. Results and Discussion

3.1. Parallel Pyrrole Adsorption on Mo(110). Parallel adsorption was initially studied, as it is generally believed pyrrole adsorbs on the surface in a flat-on geometry at low coverages.[25−28] Figure 2 presents initial and optimized parallel adsorption modes with the calculated adsorption energies. Table 1 summarizes pyrrole interatomic bond lengths, and Table 2 summarizes the interatomic bond angles for all optimized structures. The initial configurations include a flat-center mode (Pyr1) where the center of pyrrole is directly atop a Mo atom as η^5-Pyr-0°, a flat-hollow mode (Pyr2) where the center of pyrrole is directly atop a hollow site as μ_4,η^6(N,C2,C3,C3,C4,C5)-Pyr-0°, a flat-on mode with the pyrrolic nitrogen directly atop a Mo atom (Pyr3) as μ_3,η^5-Pyr-0°, a flat-on mode with the pyrrolic nitrogen atop a hollow site (Pyr4) as μ_3,η^4(C2,C3,C4,C5)-Pyr-0°, and a flat-on mode with the pyrrolic nitrogen directly atop a Mo bridge (Pyr5) as μ_4,η^6(N,N,C2,C3,C4,C5)-Pyr-0°.

Pyrrole adsorption with the center of pyrrole directly atop a Mo atom as η^5-Pyr-0° resulted in η^2(C4,C5)-Pyr-23° tilted configuration with an adsorption energy of −9.4 kcal mol^{-1} (Pyr1), the lowest adsorption energy among all studied parallel adsorption geometries. During Pyr1 optimization, pyrrole was slightly repulsed from the Mo(110) surface, and the greatest repulsion came from the nitrogen atom that moved 0.7 Å away from the Mo(110) surface from the initial position. Examination of this adsorption mode indicates possible electrophilic attack, as the C4═C5 π-orbital represents the highest occupied molecular orbital (HOMO) and is most efficient for donating electrons. The molecule shows an expansion in its interatomic bond lengths except for the N−C2 bond, which showed a reduction by 0.03 Å, while the interatomic angles within the ring showed a reduction within the C4 and C5 atoms that were involved in bonding with the Mo(110) surface. Additionally, the bond angles centered on the N, C2, and C3 atoms showed a slight expansion from their initial values (Table 2).

The Pyr2, Pyr3, and Pyr4 parallel adsorption modes resulted in similar adsorption energies of −30.7, −28.7, and −31.5 kcal mol^{-1}, respectively, all of which are higher in comparison to Pyr1. Both Pyr2 and Pyr4 optimized adsorption modes resulted in optimized geometries of μ_3,η^5-Pyr-0° with the Mo(110) surface. In both geometries, pyrrole shifts from its initial location to locate the π-orbital directly atop a Mo atom. While all of the hydrogen atoms were repulsed away from the surface, the pyrrole molecular plane remained nearly parallel to the Mo-(110) surface. It should be noted that in both of these adsorption geometries, although Pyr2 has initially five bonds with the surface through four Mo atoms and Pyr4 has four bonds with three Mo atoms, both adsorption modes resulted in μ_3,η^5-Pyr-0° optimized geometries with similar adsorption energies. Structure Pyr5 resulted in an optimized geometry of μ_2,η^2(C3,C5)-Pyr-16° tilted configuration with an adsorption energy of −19.4 kcal mol^{-1}, which is higher than structure Pyr1 and lower compared to the other optimized parallel adsorption modes. Although during optimization structure Pyr5 showed a similar interaction with the Mo(110) surface as structures Pyr2 and Pyr4, structure Pyr5 bonded through two different HOMO orbitals which contribute to the higher adsorption energy of Pyr5
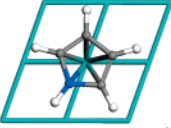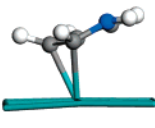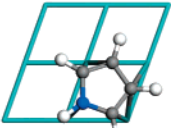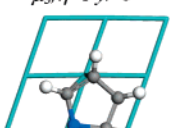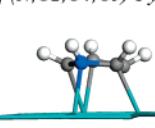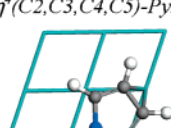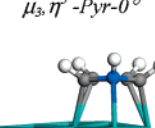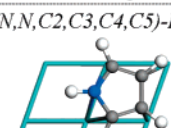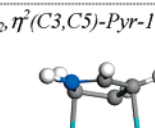
Figure 2. Initial and optimized geometries of parallel pyrrole adsorption on Mo(110) and corresponding adsorption energies.

TABLE 1: Calculated Pyrrole Bond Lengths

	optimized geometry	d(N−C2) (Å)	d(C2−C3) (Å)	d(C3−C4) (Å)	d(C4−C5) (Å)	d(C5−N) (Å)
	gas phase	1.38	1.38	1.42	1.39	1.38
Pyr1	η^2(C4,C5)-Pyr-23°	1.35 (−0.03)	1.40 (0.02)	1.46 (0.04)	1.47 (0.08)	1.43 (0.05)
Pyr2	μ_3,η^5-Pyr-0°	1.45 (0.07)	1.46 (0.08)	1.47 (0.05)	1.46 (0.07)	1.45 (0.07)
Pyr3	μ_3,η^4(N,C2,C4,C5)-Pyr-0°	1.46 (0.08)	1.48 (0.10)	1.46 (0.04)	1.43 (0.04)	1.45 (0.07)
Pyr4	μ_3,η^5-Pyr-0°	1.45 (0.07)	1.47 (0.09)	1.47 (0.05)	1.46 (0.07)	1.45 (0.07)
Pyr5	μ_2,η^2(C3,C5)-Pyr-16°	1.36 (−0.02)	1.39 (0.01)	1.46 (0.04)	1.48 (0.09)	1.43 (0.05)
Pyr6	η^2(C3,C4)-2H-Pyl-88°	1.37 (−0.01)	1.37 (−0.01)	1.52 (0.10)	1.37 (−0.02)	1.37 (−0.01)
Pyr7	μ_2,η^2(C4,C5)-2H-Pyl-81°	1.37 (−0.01)	1.36 (−0.02)	1.45 (0.03)	1.46 (0.07)	1.38
Pyr8	μ_2,η^3(N,C5,C5)-2H-Pyl-86°	1.36 (−0.02)	1.39 (0.01)	1.39 (−0.03)	1.41 (0.02)	1.42 (0.04)
Pyr9	η^1(N))-H-Pyl-84°	1.38	1.37 (−0.01)	1.41 (−0.01)	1.37 (−0.02)	1.38
Pyr10	μ_2,η^2(C2,C2)-H-Pyl-66°	1.40 (0.02)	1.42 (0.04)	1.40 (−0.02)	1.38 (−0.01)	1.35 (−0.03)
Pyr11	μ_3,η^4(C3,C3,C4,C4)-2H-Pyl-76°	1.36 (−0.02)	1.38	1.46 (0.04)	1.39	1.37 (−0.01)
Pyr12	μ_2,η^2(C4,C5)-2H-Pyl-84°	1.37 (−0.01)	1.37 (−0.01)	1.44 (0.02)	1.48 (0.09)	1.37 (−0.01)
Pyr13	μ_3,η^3(N,C5,C5)-2H-Pyl-45°	1.41 (0.03)	1.42 (0.04)	1.40 (−0.02)	1.39	1.36 (−0.02)
Pyr14	μ_2,η^2(N,C4)-H-Pyl-13°	1.37 (−0.01)	1.42 (0.04)	1.42	1.45 (0.07)	1.40 (0.02)
Pyr15	μ_3,η^4(N,C2,C3,C4)-Pyr-5°	1.36 (−0.02)	1.38	1.46 (0.04)	1.39	1.37 (−0.01)

compared to Pyr1. During optimization, the Pyr5 structure clearly shifts and rotates from its initial position while the pyrrolic nitrogen is directly atop a Mo bridge site and is slightly repulsed from the surface. The apparent repulsion of the pyrrolic nitrogen would result in a slightly lower adsorption energy, as observed comparing structures Pyr5 to structures Pyr2 and Pyr4.

Examining all optimized parallel adsorption geometries and calculated adsorption energies, structures Pyr2 and Pyr4 are most likely to occur in comparison to the other parallel structures. Although the initial adsorption geometry in these two models was different, both models resulted in an optimized μ_3,η^5-Pyr-

0° configuration. This type of interaction reflected strongly on the molecular structure of adsorbed pyrrole without destroying its aromaticity or cleaving any hydrogen bonds. The interatomic bond lengths within the ring showed relatively uniform bond length and an expansion in the hetroatom angle to an equivalent degree of other carbon atoms within the ring. Structure Pyr3 is initially positioned such that the pyrrolic nitrogen is directly atop a surface Mo atom, and evolves into a structure that is similar to Pyr2 and Pyr4 with a slightly lower adsorption energy. However, since the adsorption energies of the Pyr2, Pyr3, and Pyr4 optimized configurations are within the relative uncertainty

TABLE 2: Calculated Pyrrole Bond Angles

	∠(N−C2−C3) (deg)	∠(C2−C3−C4) (deg)	∠(C2−C4−C5) (deg)	∠(C2−C5−N) (deg)	∠(C5−N−C2) (deg)
gas phase	107.48	107.46	107.60	107.39	110.06
Pyr1	109.29 (1.81)	108.42 (0.96)	103.79 (−3.81)	105.45 (−1.94)	109.45 (−0.61)
Pyr2	108.69 (1.21)	107.55 (0.09)	107.29 (−0.31)	108.86 (1.47)	107.45 (−2.61)
Pyr3	109.91 (2.43)	106.83 (−0.63)	107.31 (−0.29)	103.56 (−3.83)	111.68 (1.62)
Pyr4	108.80 (1.32)	107.02 (−0.44)	107.37 (−0.23)	108.61 (1.22)	107.52 (−2.54)
Pyr5	105.72 (−1.76)	108.20 (0.74)	106.50 (−1.10)	109.09 (170)	108.02 (−2.04)
Pyr6	108.16 (0.68)	106.84 (−0.62)	104.38 (−3.22)	109.59 (2.20)	111.00 (0.94)
Pyr7	109.83 (2.35)	107.53 (0.07)	106.08 (−1.52)	105.54 (−1.85)	110.91 (0.85)
Pyr8	109.67 (2.19)	107.58 (0.12)	108.24 (0.64)	106.22 (−1.17)	108.27 (−1.79)
Pyr9	107.48	107.47 (0.01)	107.59 (−0.01)	107.39	110.06
Pyr10	102.56 (−4.92)	110.36 (2.90)	106.63 (−0.97)	108.37 (0.98)	112.06 (2.00)
Pyr11	108.12 (0.64)	107.05 (−0.41)	105.79 (−1.81)	108.12 (0.73)	110.59 (0.53)
Pyr12	109.67 (2.19)	108.19 (0.73)	104.90 (−2.70)	105.95 (−1.44)	110.90 (0.84)
Pyr13	109.15 (1.67)	107.04 (−0.42)	108.67 (1.07)	105.49 (−1.90)	109.44 (−0.62)
Pyr14	111.85 (4.37)	106.65 (−0.81)	104.92 (−2.68)	110.23 (2.84)	105.59 (−4.47)
Pyr15	104.53 (−2.95)	109.60 (2.14)	105.85 (−1.75)	108.17 (0.78)	108.92 (−1.14)

of the total energy calculations (1.2 kcal mol⁻¹), there is no significant difference between the adsorption energies of these structures. Thus, on the basis of adsorption energies, the preferred adsorption geometry in parallel configuration would be in the following order: Pyr2 ≈ Pyr3 ≈ Pyr4 > Pyr5 > Pyr1. This would indicate pyrrole adsorbs preferentially on Mo(110) as μ_3,η^5-Pyr-0°, and structures Pyr1 and Pyr5 are local energy minima on the potential energy surface. Furthermore, during parallel pyrrole adsorption the Mo(110) surface acts as a Lewis acid and does not promote hydrogen abstraction. These observations are in agreement with the adsorption energies and apparent lack of gas-phase H₂ from our earlier study using temperature-programmed desorption (TPD) and Auger electron spectroscopy (AES).[19]

3.2. Perpendicular and Inclined Pyrrole Adsorption on Mo(110). To elucidate all possible adsorption modes on Mo-(110), perpendicular and tilted configurations were also studied. Perpendicular structures were initially modeled with molecular pyrrole approaching the Mo(110) surface from the N−H and all C−H locations (structures not shown). The results clearly indicated these adsorption configurations were unstable and did not result in surface bonding. The observed repulsive effect resulted in all adsorption geometries moving away from the Mo-(110) surface an additional 1.5−1.7 Å from the initial distance of 2.2 Å. Therefore, perpendicular and tilted adsorption modes were studied by abstracting either one or two hydrogen atoms from pyrrole, with the resulting pyrrolyl fragment and hydrogen atom(s) bonding to the Mo(110) surface.

Figure 3 summarizes five different perpendicular configurations where all molecules are located at the same surface position and pyrrolyl approaches the surface from the C3−C4 bond (η^2-(C3,C4)-2H-Pyl-90°, structure Pyr6), C4═C5 double bond (η^2-(C4,C5)-2H-Pyl-90°, structure Pyr7), and both C5 and N after abstracting two hydrogen atoms and bonding both on the surface (η^2(N,C5)-2H-Pyl-90°, structure Pyr8). Structure Pyr6 resulted in an adsorption energy of −9.6 kcal mol⁻¹, the lowest adsorption energy of all perpendicular pyrrolyl geometries studied. The optimized structure retained its initial adsorption geometry without noticeable changes in its structure or position, although it did bend slightly toward the surface by 2° to form an η^2-(C3,C4)-2H-Pyl-88° configuration. Structure Pyr7 resulted in the highest adsorption energy with a value of −55.3 kcal mol⁻¹. During optimization, pyrrolyl shifts from its initial position and bends toward the surface such that the other π-orbital (C2═C3) tries to bond with the surface as μ_2,η^2(C4,C5)-2H-Pyl-81°. The interatomic bond lengths showed an increase by 0.07 Å for the C4−C5 bond, and only slight changes to other bonds. The high adsorption energy in this case was the result of a strong

interaction between the molecule through its HOMO orbitals and the surface. Structure Pyr8 produced an adsorption energy of −30.3 kcal mol⁻¹ with an optimized bonding geometry of μ_2,η^3(N,C5,C5)-2H-Pyl-86°. During optimization, pyrrolyl migrates from its initial position atop a Mo atom to directly above a hollow site. The ring structure showed slight deformation as indicated by the changes in the interatomic bond lengths and angles, as shown in Tables 1 and 2, respectively.

In addition to the previous perpendicular adsorption modes, two additional configurations were studied by abstracting the hydrogen atom from the pyrrolic nitrogen initially bonding as η^1(N)-H-Pyl-90° (structure Pyr9), and by abstracting an α-C hydrogen atom initially bonding as η^1(C2)-H-Pyl-90° (structure Pyr10). In both adsorption modes, the pyrrolyl fragment approached the Mo(110) surface directly atop a Mo atom. For structure Pyr9, the number and type of bonds did not change considerably following optimization: the optimized structure shows a slight attraction between the molecular plane and the surface, forming a slightly tilted configuration as η^1(N)-H-Pyl-84° with an adsorption energy of −17.4 kcal mol⁻¹. However, during optimization structure Pyr10 shifted from the initial position and resulted in an optimized geometry of μ_2,η^2(C2,-C2)-H-Pyl-66° with an adsorption energy of −24.2 kcal mol⁻¹.

The initial and optimized pyrrolyl adsorption configurations with the molecular plane inclined with respect to the Mo(110) surface are presented in Figure 4. These configurations are similar to the previously discussed perpendicular pyrrolyl adsorption configurations, except the pyrrolyl molecular plane was inclined 45° with respect to the Mo(110) surface as η^2-(C3,C4)-2H-Pyl-45° (structure Pyr11), η^2(C4,C5)-2H-Pyl-45° (structure Pyr12), and η^2(N,C5)-2H-Pyl-45° (structure Pyr13). Two additional configurations were studied at inclination angles of 15° to the Mo(110) surface as μ_3,η^5-H-Pyl-15° (structure Pyr14) pyrrolyl adsorption and μ_3,η^5-Pyr-15° (structure Pyr15) molecular pyrrole adsorption. During Pyr11 optimization, the C3−C4 σ-orbital shifts from the initial location directly atop a Mo atom to a hollow site bonding to three Mo atoms. The pyrrolyl plane angle with the Mo(110) surface increases from 45° to 76°, forming a μ_3,η^4(C3,C3,C4,C4)-2H-Pyl-76° configuration with an adsorption energy of −31.3 kcal mol⁻¹. Both Pyr12 and Pyr13 configurations showed similar adsorption energies of −37.4 and −36.9 kcal mol⁻¹, respectively. However, while Pyr13 maintained a 45° angle with respect to the Mo-(110) surface, structure Pyr12 increased the angle of inclination to 84° and shifted its initial position from atop a Mo atom to a hollow site as μ_2,η^2(C4,C5)-2H-Pyl-84°. Structure Pyr12 also showed an expansion in the interatomic bond length involving C4, while the other bonds changed only slightly. This is also

Model	Adsorption Energy [kcal mol^{-1}]	Initial Geometry	Optimized Geometry
Pyr6	-9.6	*η²(C3,C4)-2H-Pyl-90°*	*η²(C3,C4)-2H-Pyl-88°*
Pyr7	-55.3	*η²(C4,C5)-2H-Pyl-90°*	*μ₂,η²(C4,C5)-2H-Pyl-81°*
Pyr8	-30.3	*η²(N,C5)-2H-Pyl-90°*	*μ₂,η³(N,C5,C5)-2H-Pyl-86°*
Pyr9	-17.4	*η¹(N)-H-Pyl-90°*	*η¹(N))-H-Pyl-84°*
Pyr10	-24.2	*η¹(C2))-H-Pyl-90°*	*μ₂,η²(C2,C2)-H-Pyl-66°*

Figure 3. Initial and optimized geometries of perpendicular pyrrole and pyrrolyl adsorption on Mo(110) and corresponding adsorption energies.

reflected in the interatomic bond angles, where the angle centered on C4 showed a reduction by 2.7°. During the optimization of Pyr13, pyrrolyl rotates in such a way that the pyrrolic N positions directly atop a Mo atom. The molecule retains a similar angle with respect to the Mo(110) surface with an optimized configuration of μ_3,η^3(N,C5,C5)-2H-Pyl-45°. Structure Pyr14 did not change considerably upon optimization, and formed a μ_2,η^2(N,C4)-H-Pyl-13° structure with a corresponding adsorption energy of −31.4 kcal mol^{-1}. In the final configuration Pyr15, which is similar to Pyr14 except the N−H is not cleaved and pyrrole is adsorbed molecularly, the optimized configuration showed a lower adsorption energy of −29.9 kcal mol^{-1}. The angle of inclination was also slightly reduced and bonded to the Mo(110) surface as μ_3,η^4(N,C2,C3,C4)-Pyr-5°.

Based on the relative adsorption energies of the perpendicular and tilted adsorption configurations on Mo(110), structure Pyr7 showed the highest stability among the configurations studied. This indicates that the Pyr7 structure is the most energetically favorable if Mo(110) promotes hydrogen abstraction to form pyrrolyl species. This is consistent with the electronic structure of pyrrole whereby pyrrole is an electron-rich molecule that reacts readily with electrophiles but is not susceptible to nucleophilic attack. In comparison with the tilted models as shown in Figure 4, tilted adsorption did not show stability similar to that of structure Pyr7. However, tilted adsorption did result in adsorption energies comparable to those of pyrrolyl adsorption (structures Pyr10, Pyr11, Pyr12, and Pyr13) or molecular pyrrole adsorption (structure Pyr15). Thus, it is reasonable to suggest

that pyrrole may adsorb perpendicular to the surface after abstracting hydrogen atoms from the approaching side, similar to structure Pyr7. It should be noted that previous experimental investigations of pyrrole adsorption and decomposition on Mo-(110)[19] did not indicate gas-phase H$_2$ as a decomposition product. On the basis of this observation, pyrrole adsorption as pyrrolyl species following hydrogen abstraction is not likely to occur on Mo(110). Therefore, structure Pyr15 with an adsorption energy similar to that of parallel pyrrole adsorption would be the preferred adsorption model for perpendicular and tilted pyrrole adsorption.

The possibility of forming a tilted adsorbed species through phase transformation from parallel adsorption was studied by calculating the activation energy barrier using the optimized models of Pyr2, Pyr3, and Pyr4 as initial geometries. The activation energies were in the range of 160−250 kcal mol^{-1}, which are significant compared to the relative adsorption energies for parallel adsorption (28.7−31.5 kcal mol^{-1}). Thus, it is clearly not possible for this type of geometric transformation to occur on Mo(110) during the course of increasing surface temperature.

3.3. Coverage-Dependent Pyrrole Adsorption on Mo(110). Pyrrole adsorption on Mo(110) was studied as a function of surface coverage to gain additional insight into the effects of lateral interactions between pyrrole molecules during adsorption. Three models including two, three, and four pyrrole molecules per unit cell were initially constructed in a parallel adsorption configuration as shown in Figure 5. In the case of two pyrrole

Model	Adsorption Energy [kcal mol^{-1}]	Initial Geometry	Optimized Geometry
Pyr11	-31.3	η^2(C3,C4)-2H-Pyl-45°	μ_3,η^4(C3,C3,C4,C4)-2H-Pyl-76°
Pyr12	-37.4	η^2(C4,C5)-2H-Pyl-45°	μ_2,η^2(C4,C5)-2H-Pyl-84°
Pyr13	-36.9	η^2(N,C5)-2H-Pyl-45°	μ_3,η^3(N,C5,C5)-2H-Pyl-45°
Pyr14	-31.4	μ_3,η^5-H-Pyl-15°	μ_2,η^2(N,C4)-H-Pyl-13°
Pyr15	-29.9	μ_3,η^5-Pyr-15°	μ_3,η^4(N,C2,C3,C4)-Pyr-5°

Figure 4. Initial and optimized geometries of inclined pyrrole and pyrrolyl adsorption on Mo(110) and corresponding adsorption energies.

molecules adsorbing on Mo(110) (Pyrrole-2M), both molecules showed a combination of initial N atom repulsion from the surface and some lateral interaction with a total adsorption energy of −35.7 kcal mol^{-1}. Adsorbate−adsorbate interactions caused the molecules to bond in different configurations: one as η^2(C4,C5)-Pyr-26° and the other as μ_3,η^4(N,C2,C4,C5)-Pyr-0°. In the case of the three-pyrrole model (Pyrrole-3M), the optimization showed initial repulsive forces between the Mo-(110) surface and the molecules, as well as considerable lateral interactions that result in two pyrrole molecules tilting and interacting with the surface through HOMO orbitals in an opposite molecular plane direction as η^1(C2)-Pyr-tilted and μ_2,η^2(C4,C5)-Pyr-tilted, respectively. The third molecule had less interaction with the other molecules and showed less tilting effect. The bonding mode formed in this case was μ_3,η^4(N,-C2,C4,C5)-Pyr-0°, and the nitrogen atom moved up in a higher location than the rest of the ring. The total adsorption energy for the Pyrrole-3M configuration was −34.0 kcal mol^{-1}, and at this coverage all molecules showed significant ring deformation, particularly with the atoms involved with bonding to the Mo(110) surface. In the case of the four-pyrrole model (Pyrrole-4M), the optimization resulted in an unstable system that did not bond to the Mo(110) surface, as evidenced by a total bonding energy of +1.0 kcal mol^{-1}. The pyrrole molecules did not show any observable ring deformation, which is also consistent with pyrrole not bonding to the Mo(110) surface. One additional model was constructed (model not shown) using four pyrrole

molecules adsorbing in different modes (parallel, perpendicular, and tilted). In this configuration, only one pyrrole molecule bonded to the surface (initially set to parallel mode) in parallel position, while all other molecules did not form any bonds with the Mo(110) surface.

The coverage-dependent adsorption configurations suggest that, at high pyrrole coverages on Mo(110), the adsorption energy per pyrrole molecule is significantly reduced and the adsorption geometry is perturbed due to adsorbate−adsorbate interactions. During the adsorption of two pyrrole molecules per Mo(110) unit cell, the average pyrrole adsorption energy was −17.9 kcal per adsorbed pyrrole molecule; this adsorption energy reduces to −11.3 kcal per adsorbed pyrrole molecule for the adsorption of three pyrrole molecules. Lateral interactions between the adsorbed pyrrole molecules further destabilize pyrrole adsorption on Mo(110) at a coverage of four pyrrole molecules per unit cell, resulting in a system that did not bond to the Mo(110) surface. These results suggest that, since the adsorption energy per pyrrole molecule is lowered significantly by repulsive interactions between adsorbed pyrrole molecules, a more stable structure could evolve through the desorption of pyrrole from the surface. It should be noted, however, that the calculations use individual gas-phase pyrrole molecules in an infinite vacuum cell as an energetic reference per eq 1, and not a cluster of pyrrole molecules. The optimized geometries at higher pyrrole coverages also indicate that different adsorption modes at higher pyrrole coverages may coexist with parallel
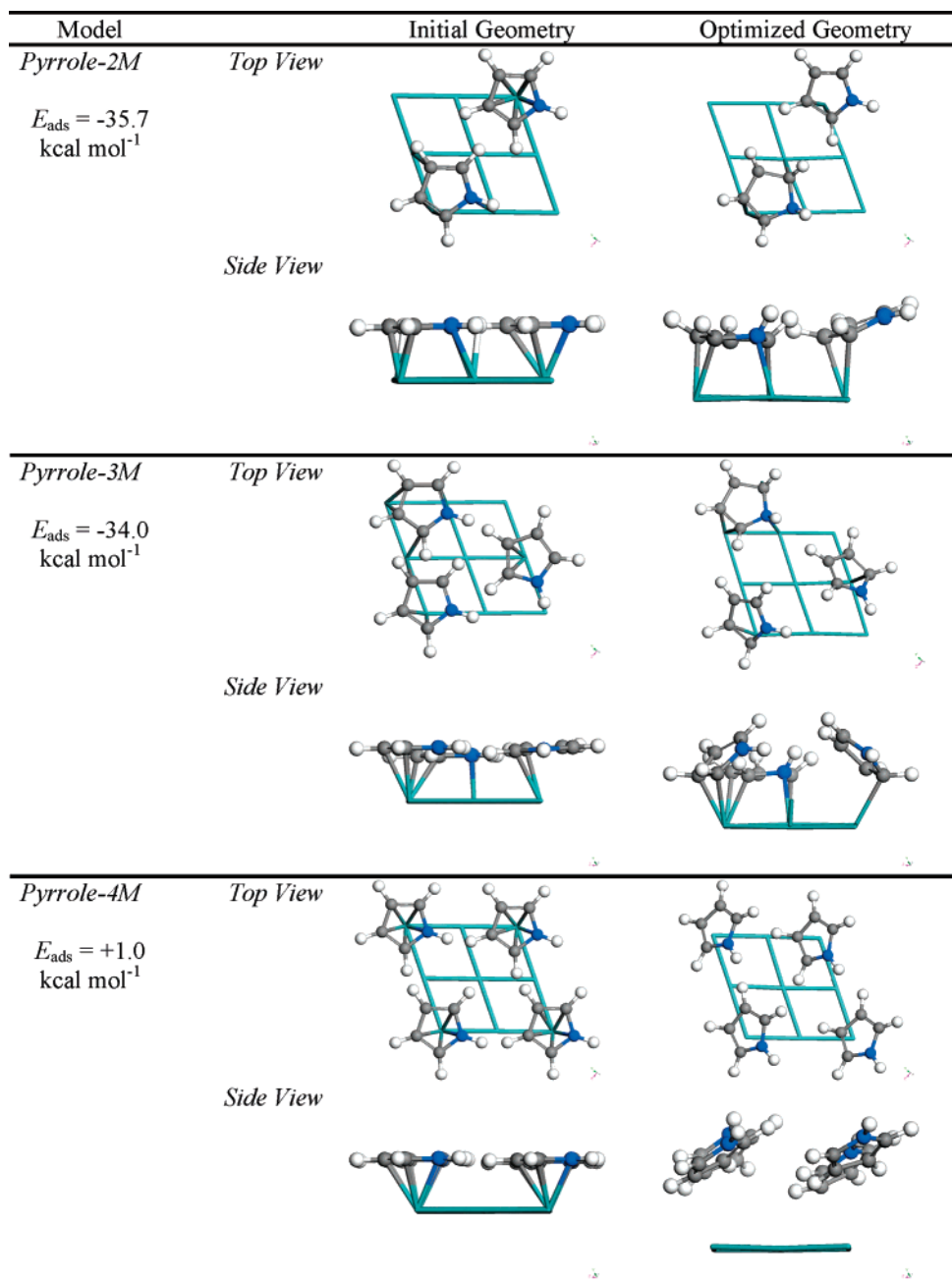
Figure 5. Initial and optimized geometries of parallel pyrrole adsorption on Mo(110) as a function of surface coverage.

pyrrole adsorption, specifically slightly tilted adsorption modes relative to the Mo(110) surface.

3.4. Implications for Mo-Based Hydrotreating Catalysts. The removal of heterocyclic nitrogen compounds through catalytic hydrotreatment proceeds via two key reaction steps: (1) hydrogenation of the heterocyclic ring, which consumes large amounts of hydrogen in comparison to hydrodesulfurization since the latter does not require hydrogenation,[29] and (2) C−N bond scission, which is suggested to occur through either Hofmann-type elimination or nucleophilic substitution followed by C−S hydrogenolysis.[30] It is generally believed that basic organonitrogen compounds interact with the active sites over the catalyst surface by two adsorption modes, including parallel adsorption through the π-ring and perpendicular adsorption through the nitrogen atom. In contrast, nonbasic organonitrogen compounds cannot interact through the pyrrolic nitrogen due to steric hindrance of the hydrogen atom bonded to the pyrrolic nitrogen.

In our previous study of pyrrole adsorption and decomposition on Mo(110), one desorption feature was observed with an apparent first-order activation energy of 21.9 ± 0.6 kcal mol^{-1}, and it was suggested that this single desorption feature was attributed to parallel adsorption via π-orbital interaction without any hydrogen bond cleavage. This was based on the absence of desorbing hydrogen and a direct comparison to pyrrole adsorption on other surfaces. Experimental studies of pyrrole adsorption and reaction on Mo(110),[19] Cu(100),[31] and Pt(111)[32] have not reported additional reaction products desorbing from the surface, while studies on Rh(111),[33] Pd(111),[34] and Ni(100)[35] have reported hydrogen, ammonia, and hydrogen cyanide as major products. In these studies, there was some attempt to suggest possible adsorption modes for pyrrole, in particular at low coverage, which tends to be generally accepted as parallel adsorption with respect to the metal surface. However, none explained the exact adsorption configuration that is responsible for such behavior.

The present results indicate that pyrrole adsorption on Mo-(110) occurs via parallel adsorption (Pyr2, Pyr3, and Pyr4), with the possibility of slightly tilted modes similar to Pyr15 at higher coverages due to adsorbate−adsorbate interactions. Perpendicular structures modeled with molecular pyrrole approaching the Mo(110) surface from all N−H and all C−H locations were unstable and did not result in surface bonding. While pyrrolyl adsorption is energetically possible, these adsorption modes are only possible following hydrogen abstraction. The present work has indicated that Mo(110) does not demonstrate hydrogen abstraction tendencies, which is consistent with our previous experimental studies that did not detect hydrogen desorbing from Mo(110). Furthermore, the optimized parallel adsorption modes required three Mo coordination sites (i.e., μ_3,η^5-Pyr-0° and μ_3,η^4-(N,C2,C4,C5)-Pyr-0°), regardless of initial geometry. The average calculated adsorption energy for parallel pyrrole adsorption was 30.3 kcal mol^{-1}, which is similar to the apparent first-order activation energy previously estimated by the Redhead equation.[36]

Basic and nonbasic organonitrogen adsorption is readily facilitated on Mo(110) due to the long-range order of the surface. However, the active sites on Mo-based hydrotreating catalyst surfaces are limited since these active sites are located on the edge planes on MoS$_2$ clusters. Basic organonitrogen compounds have the tendency to adsorb through the nitrogen atom that requires one Mo site, while nonbasic organonitrogen compounds tend to require three Mo sites to facilitate parallel adsorption. These differences in adsorption modes and the availability of active sites can partly explain the relative differences in activity between basic and nonbasic organonitrogen compounds during catalytic hydrotreatment.[37]

4. Conclusions

On the basis of the DFT calculations for the adsorption of pyrrole on Mo(110), it is suggested that pyrrole adsorbs molecularly on the surface in a parallel mode through its π-orbitals without cleaving any hydrogen atoms, similar to Pyr2, Pyr3, and Pyr4 models with an adsorption energy of −28.7 to −31.5 kcal mol^{-1}. These adsorption models resulted in flat-lying pyrrole bonding to three Mo atoms as μ_3,η^5-Pyr-0° (structures Pyr2 and Pyr4) or μ_3,η^4(N,C2,C4,C5)-Pyr-0° (structure Pyr3). As the surface exposure increases, lateral interactions between pyrrole molecules during adsorption are suggested to cause competitive adsorption resulting in the coexistence of slightly tilted pyrrole molecules bonding to the surface along with parallel adsorption configurations. This slightly tilted configuration can be assigned to a μ_3,η^4(N,C2,C3,C4)-Pyr-5° (structure Pyr15) bonding mode with an adsorption energy of −29.9 kcal mol^{-1}. These slightly tilted adsorption configurations are a result of molecular interaction and not the result of phase transformation on the surface. Additional analysis of pyrrole adsorption on Mo(110) is currently being performed using high-resolution electron energy loss spectroscopy to further study pyrrole molecular orientation and bond rehybridization.

References and Notes

(1) Young, E. C.; Maeng, J. Y.; Sehun K. *J. Am. Chem. Soc.* **2003**, *125*, 7514.

(2) Mate, C. M.; Somorjai, G. A.; Tom, H. W.; Zhu, X. D.; Shen, Y. R. *J. Chem. Phys.* **1988**, *88*, 441.

(3) Abdallah, W. A.; Nelson, A. E.; Gray, M. R. *Surf. Sci.* **2004**, *569*, 193.

(4) Whitten, J. E. *Surf. Sci.* **2003**, *546*, 107.

(5) Andersson, M. P.; Uvdal, P. *J. Phys. Chem. B* **2001**, *105*, 9458.

(6) Grassian, V. H.; Muetterties, E. L. *J. Phys. Chem.* **1987**, *91*, 389.

(7) Jorgebsen, W. L.; Salem, L. *The Organic Chemist's Book of Orbitals*; Academic Press: New York, 1973.

(8) Jones, R. A.; Bean, G. P. *The Chemistry of Pyrroles*; Academic Press: New York, 1977.

(9) DuBois, M. R.; Vasquez, L. D.; Ciancanelli, R. F.; Noll, B. C. *Organometallics* **2000**, *19*, 3507.

(10) Sanchez-Delgado, R. A. *Organometallic Modelling of the Hydrodesulfurization and Hydrodenitrogenation Reactions*; Kluwer: Dordrecht,The Netherlands, 2002.

(11) Kvietov, F.; Allured, V.; Carperos, V.; Dubois, M. R. *Organometallics* **1994**, *13*, 60.

(12) Fish, R. H.; Baralt, E.; Kim, H. S. *Organometallics* **1991**, *10*, 1965.

(13) Felkin, H.; Zakrzewski, J. *J. Am. Chem. Soc.* **1985**, *107*, 3374.

(14) Efraty, A.; Jubran, N.; Goldman, A. *Inorg. Chem.* **1982**, *21*, 868.

(15) Glueck, D. S.; Hollander, F. J.; Bergman, R. G. *J. Am. Chem. Soc.* **1989**, *111*, 2719.

(16) Cordone, R.; Harman, W. D.; Taube, H. *J. Am. Chem. Soc.* **1989**, *111*, 5959.

(17) Myers, W. H.; Sabat, M.; Harman, W. D. *J. Am. Chem. Soc.* **1991**, *113*, 6682.

(18) Bianchini, C.; Meli, A.; Vizza, F. *Eur. J. Inorg. Chem.* **2001**, *1*, 43.

(19) Abdallah, W. A.; Nelson, A. E. *Surf. Sci.* **2005**, in press.

(20) Perdew, J. P.; Burke, K.; Ernzerhof, M. *Phys. Rev. Lett.* **1996**, *77*, 3865.

(21) Perdew, J. P.; Wang, Y. *Phys. Rev. B* **1992**, *45*, 3244.

(22) Monkhorst, H. J.; Pack, J. D. *Phys. Rev. B* **1976**, *13*, 5188.

(23) Vanderbildt, D. *Phys. Rev. B* **1990**, *41*, 7892.

(24) Pulay, P. *Mol. Phys.* **1969**, *17*, 197.

(25) Sexton, B. A. *Surf. Sci.* **1985**, *163*, 99.

(26) Schoofs, G. R.; Benziger, J. B. *Surf. Sci.* **1987**, *191*, 373.

(27) Netzer, F. P.; Bertel, E.; Goldmann, A. *Surf. Sci.* **1988**, *199*, 87.

(28) Baddeley, C. J.; Hardacre, C.; Ormerod, R. M.; Lambert, R. M. *Surf. Sci.* **1996**, *369*, 1.

(29) Kabe, T.; Ishihara, A.; Qian, W. *Hydrodesulfurization and Hydrodenitrogenation: Chemistry and Engineering*; Kodansha Ltd.: Tokyo, 1999.

(30) Prins, R. *Adv. Catal.* **2001**, *46*, 399.

(31) Sexton, B. A. *Surf. Sci.* **1985**, *163*, 99.

(32) Tourillon, G.; Raaen, S.; Skotheim, T. A.; Sagurton, M.; Garrett, R.; Williams, G. P. *Surf. Sci.* **1987**, *184*, L345.

(33) Netzer, F. P.; Bertel, E.; Goldmann, A. *Surf. Sci.* **1988**, *199*, 87.

(34) Baddeley, C. J.; Hardacre, C.; Ormerod, R. M.; Lambert, R. M. *Surf. Sci.* **1996**, *369*, 1.

(35) Schoofs, G. R.; Benziger, J. B. *Surf. Sci.* **1987**, *191*, 373.

(36) Redhead, P. A. *Vacuum* **1962**, *12*, 203.

(37) Frost, C. M.; Jensen, H. B. *Prepr.−Am. Chem. Soc., Div. Pet. Chem.* **1973**, *18*, 119.